JOURNAL OF MATERIALS SCIENCE 28 (1993) 3161–3167

Spillover effect in the hydrogen absorption by the polycrystalline powder alloy $FeNi_{1.75}Cu_{1.5}Mo_{0.5}$ and electric conductivity of the pressed powder

M. V. ŠUŠIĆ
Faculty of Physical Chemistry, University of Belgrade, PO Box 550, YU-11001 Belgrade, Yugoslavia

A. M. MARIČIĆ
Technical Faculty, B. Kidriča 65, YU-32000 Čačak, Yugoslavia

The process of hydrogen absorption by the $FeNi_{1.75}Cu_{1.5}Mo_{0.5}$ alloy in the polycrystalline form was investigated for both the pure and palladized forms (0.008 76% Pd) at temperatures from ambient to 600 °C in a hydrogen flow. Using differential scanning calorimetry, (DSC) thermogravimetry (TG) and X-ray diffraction, the influence of palladization on the hydrogen absorption was demonstrated. Kinetic analysis of the DSC thermograms, the kinetic and thermic parameters of hydrogen absorption were determined. The TG thermograms showed that on hydrogen absorption a weight change took place due to water formation and reduction of the oxide film at the surface of the powder particles. The activation energies of hydrogen absorption were 170 kJ mol^{-1} for the original powder and 32 kJ mol^{-1} for the palladized one. The enthalpies of the absorption ranged from $\Delta H = -5$ to $\Delta H = -380$ J g^{-1} for the original and palladized powder, respectively. The rate constants of the absorption depended on the palladization and were found to be 0.03 and 1.20 s^{-1}, respectively, at 162 °C. The electric conductivity of the pressed powder (9 kbar) increases on heating in both air and a hydrogen atmosphere up to 600 °C, tending to a constant value. The changes of the parameters characteristic of the palladized form are ascribed to the mechanism of a hydrogen spillover effect due to the presence of palladium.

1. Introduction

Under different conditions many metals, alloys and intermetallic compounds absorb hydrogen which often dissolves as an interstitial component of the system. This effect may be interesting from the energetic and technological points of view [1, 2]. In addition, hydrides of some intermetallic compounds could be used as sensory and regulatory systems [3, 4]. Recent investigations show an increasing interest in multicomponent alloys which absorb hydrogen over a wide temperature range and under differing hydrogen pressures. By coupling two or more of these metal hydrides, it is possible to develop devices for various applications. In the design of control and protection equipment attention is directed towards alloys which can be hydridated at temperatures between 80 and 100 °C [5] and at hydrogen pressures of 1–2 MPa. This group of binary and ternary alloys includes $LaAl_{0.3}Ni_{4.7}$, $CeNi_5$, $TiFe_{0.85}$, $Ce_{y-x}R_xNi_{2.5}Cu_{2.5}$ (R = La, Pr, $0.5 < x < 2.5$), which are hydridated at hydrogen pressures of about 0.1–50 bar (1 bar = 10^5 Pa) [6].

The process of hydrogen absorption in metals (alloys) in the majority of cases takes place in two steps: in the first one molecular hydrogen is adsorbed at the surface, which is followed by a more or less extensive dissociation of the molecules into atoms, depending on the catalytic properties of the metal. In the second step the atomic hydrogen diffuses into the lattice of the metal where it is dissolved or bound to mono- or polyhydrides, depending on the nature of the metal (alloy). Therefore, the metals, which are poor catalysts of the $H_2 \rightarrow 2\,H$ process, at moderate hydrogen pressures show a limited absorption capacity for hydrogen. However, the presence of small amounts of dispersed palladium or platinum leads to an efficient catalysis of dissociation. The atomic hydrogen thus formed then diffuses into the lattice of the host metal, as has been demonstrated with the alloy $LaNi_4Al$–Pd [7] and with oxide bronzes WO_3–Pd and MoO_3–Pd, with a palladium content below 1%. This process of hydridation is termed hydrogen spillover [8, 9].

The penetration of hydrogen into the lattice of the metal (alloy) can considerably affect its electrical conductivity. It has been shown that with some intermetallic compounds of lanthanides and actinides, the

conductivity decreases due to a depopulation of electrons in the conduction band, the absorbed hydrogens behaving as anions [11], leading to a dominance of ionic bonds.

In the present work the hydrogen spillover effect was studied in the polycrystalline alloy $FeNi_{1.75}Cu_{1.5}Mo_{0.5}$ in the presence of minute amounts of palladium.

2. Experimental procedure

The alloy $Fe_{96.25}Ni_{1.75}Cu_{1.5}Mo_{0.5}$ (subscripts denoting percentages by weight) was obtained by spraying the alloy melt on to a sufficiently cold support, without producing a glassy state. The obtained powder contained particles of diameters below 100 nm. Measurements of the electrical conductivity were performed on samples pressed at 9 kbar in the form of square bars 10 mm long and with a base (cross-section) of 0.3 mm^2. The four-point method was applied in air or a hydrogen atmosphere, varying the temperature from ambient to 600 °C. Conductivity was monitored at steady heating or cooling in the same atmosphere. The process of hydrogen absorption was examined by differential scanning calorimetry (DSC) and thermogravimetry (TG) using a DuPont Thermal Analyser 1090, and by X-ray diffraction (XRD) with a Philips Analytical PW 710 Diffractometer, using CuK_α radiation (0.154 06 nm) .

The examinations were carried out on pure and palladized samples. The palladization was performed by soaking weighed amounts of samples in solutions of $Pd(NO_3)_2$ of known concentrations. The samples and solutions were dried and heated to 500 °C in order to decompose the nitrate. The calculated percentage of palladium in the sample investigated was 0.008 76, distributed initially on the surface of the powder particles.

3. Results and discussion

3.1. Kinetic–thermodynamic analysis of thermograms

According to Borchardt and Ferrington [12] in the nonisothermal analysis of differential enthalpy (DEA) and differential thermograms (DTA), the rate constant of the chemical reaction may be defined as

$$k = [C_p(d\Delta T/dt) + K\Delta T]/[(A - a) - C_p\Delta T] \quad (1)$$

where C_p is the reactant heat capacity, K the heat transfer coefficient, $d\Delta T/dt$ the slope of the thermogram at a certain time, t, of the process duration, A the total area of the maximum, and a the partial area under the curve up to the time t. It was shown that the terms $C_p(d\Delta T/dt)$ and $C_p\Delta T$ are, over the whole thermogram range, one order of magnitude smaller than the terms to which they are added or subtracted, and Equation 1 reduces to

$$k = \Delta T/(A - a) \quad (2)$$

This also applies to DSC thermograms, and Equation 2 can be written as

$$k = (dH/dt)/(A - a) \quad (3a)$$

or

$$k = \Delta mW/(A - a) \quad (3b)$$

where ΔmW is the change of liberated (consumed) energy in milliwatts at time t of process duration, i.e. the enthalpy change.

3.2. Hydrogen absorption by the original powder

In the hydrogen flow the original powder absorbs hydrogen very poorly in the range 25–600 °C. The enthalpy is also rather low, i.e. $\Delta H = -5$ J g^{-1} in the third hydridation, as shown by the DSC thermogram in Fig. 1. Kinetic analysis of this thermogram according to Equation 3 shows a linear dependence of log k versus $1/T$ (Fig. 2a), indicating a first-order reaction for the absorption process. The slope of the diagram yields a quite high activation energy of $E = 170 \pm 6$ kJ mol^{-1} and a high frequency factor of $Z = 3.1 \times 10^{15}$ s^{-1}. It appears as if the hydrogen absorption takes place only on the nickel component which is a small fraction of the alloy. This could explain the small magnitudes of the rate constants and the high activation energy of the absorption process.

3.3. Hydrogen absorption by the palladized powder

Hydrogen absorption by the palladized powder is shown by DSC thermograms in Fig. 3. On thermogram (a) (first hydridation) an exo maximum at 222.9 °C is seen (marked 1) indicating a small, but double absorption compared to the original powder, with an enthalpy change of $\Delta H = -11.1$ J g^{-1}. Kinetic analysis of this maximum shows two straight lines with different slopes (Fig. 4a). From the first slope, marked 1, and the second one, marked 2, activation

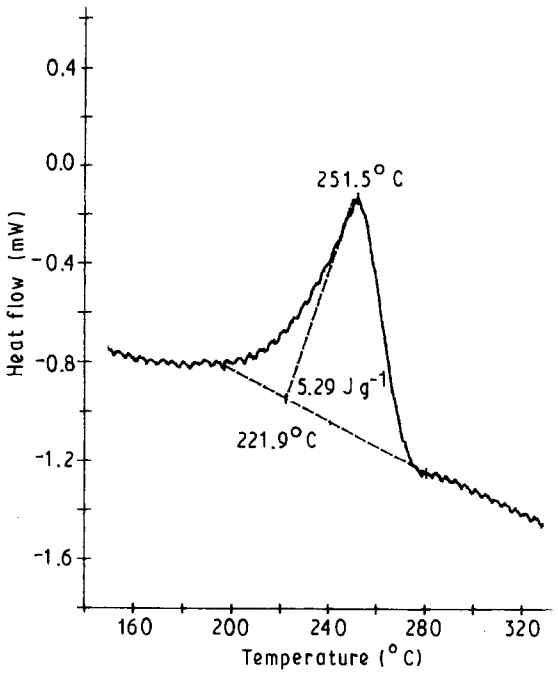

Figure 1 DSC thermogram of hydrogen absorption with the original powder in a hydrogen flow, third hydridation, 30 K min^{-1}.

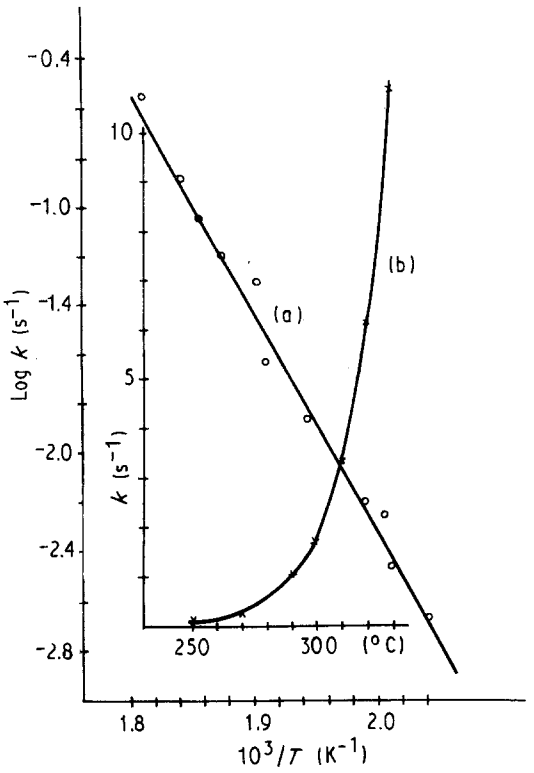

Figure 2 (a) Energy of activation plot and (b) dependence of the rate constant of absorption on temperature for the thermogram of Fig. 1.

energies of $E_1 = 69 \pm 3$ kJ mol^{-1} and $E_2 = 120 \pm 5$ kJ mol^{-1} are obtained, respectively, while the corresponding frequency factors are $Z_1 = 7.4 \times 10^6$ s^{-1} and $Z_2 = 3.3 \times 10^{12}$ s^{-1}. Curves b_1 and b_2 show the temperature dependence of the rate constants of the two separate processes, calculated using the above constants. The second step should originate from a hindered diffusion of hydrogen in the first hydridation by the end of the hydridation.

On thermogram (a) of Fig. 3, an endothermal peak, marked 2, is rather prominent with a minimum at 457 °C, showing a considerable enthalpy change of $\Delta H = 83.1$ J g^{-1}. Its origin is explained by the TG analysis, which will be described in Section 3.4.

Thermogram (b) in Fig. 3 is obtained with the same sample after cooling it in a hydrogen flow and subsequently exposing it to air for about 1 h. It can be seen that hydrogen absorption is considerably increased and takes place at a lower temperature (175 °C). This could be explained by the activation of the sample in the first hydridation. The endo minimum, marked 2, does not correspond to the minimum occurring in the first hydridation. Kinetic data for the second hydridation (thermogram b, Fig. 3) are shown in Fig. 5. An energy of activation of 32 ± 1 kJ mol^{-1} is obtained with a frequency factor of 7.7×10^3 s^{-1}.

The obtained kinetic and thermal parameters show that the presence of palladium in the sample decreases both the activation energy and the frequency factor and increases the rate constant of hydrogen take up, as seen in Figs 2 and 5, i.e. the rate constant of the process on the non-palladized sample at 435 K is 0.03 s^{-1}, while for the palladized one $k = 1.20$ s^{-1}. The temperature dependence of this constant is shown in Fig. 5.

The same sample after cooling in hydrogen and keeping in air overnight, was doubly cycled in hydrogen (without allowing contact with air). The result, shown in Fig. 6, indicates clearly that the sample becomes incompletely saturated with hydrogen in a single cycle, i.e. the activation is not terminated. The total enthalpy for two heating and cooling cycles in hydrogen (after four previous hydridations) amounts to $\Delta H = -280$ J g^{-1}.

The course of repeated hydridation of a palladized sample pressed at 8 kbar is shown by the thermograms

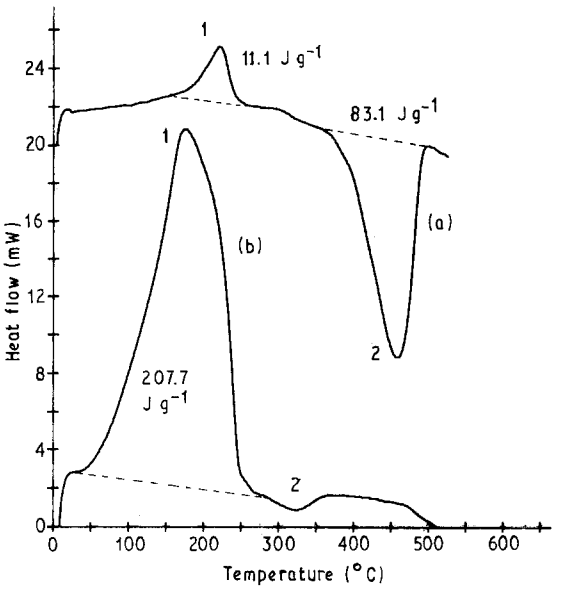

Figure 3 DSC thermogram of hydrogen absorption on the palladized sample (0.00876% Pd) : (a) first and (b) second hydridation in a hydrogen flow, 30 K min^{-1}.

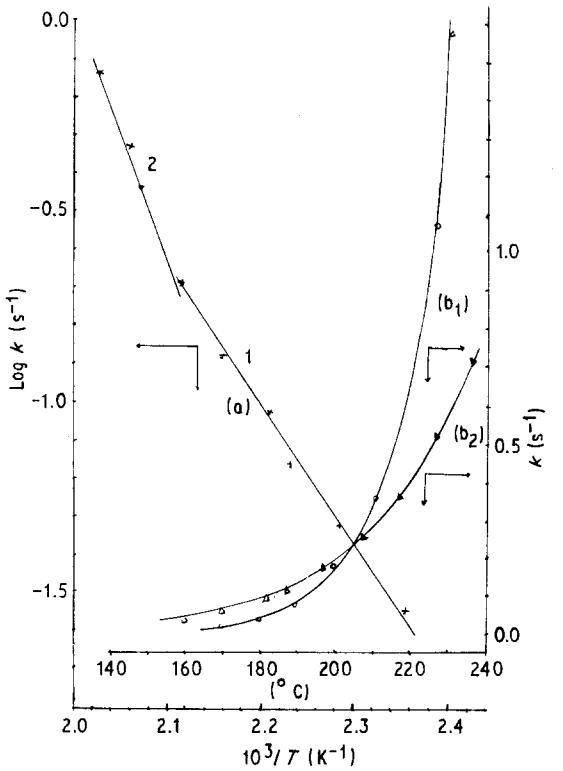

Figure 4 Energy of activation plot: (a) for the exo maximum 1 of thermogram (a) of Fig. 3; b_1 and b_2 are temperature dependences of the rate constant for the first and second stages.

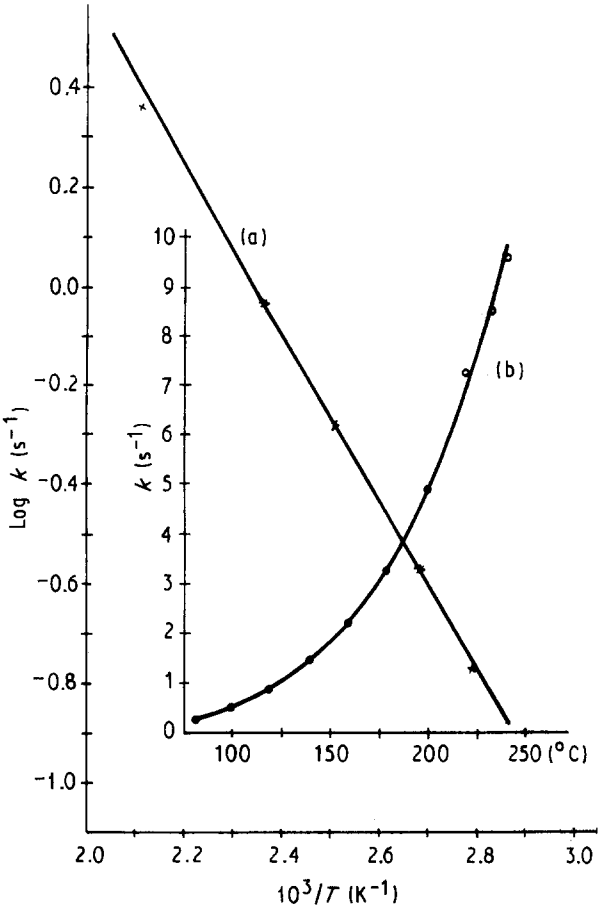

Figure 5 Energy of activation plot for exo maximum 1 of thermogram (b) of Fig. 3.

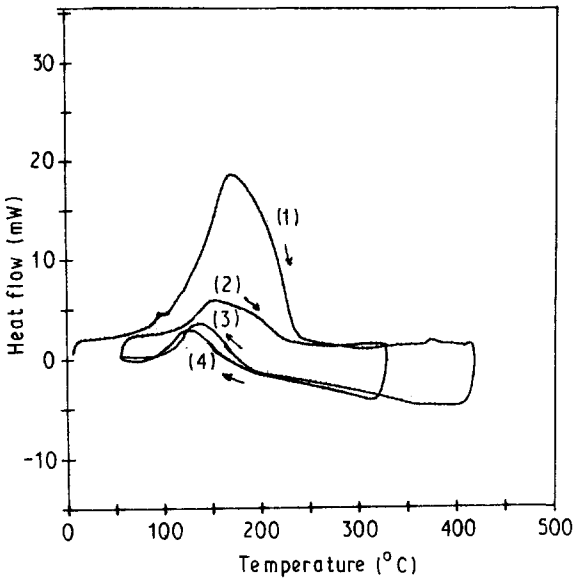

Figure 6 DSC thermogram of cyclic (heating–cooling) hydridation of the palladized powder from Fig. 3 after the fourth hydridation, cooling in hydrogen and residing in air for 20 h, 20 K min^{-1}. ΔH: (1) -198 J g^{-1}, (2) -39 J g^{-1}, (3) -25 J g^{-1}, (4) -17 J g^{-1}. Total $\Delta H = -279$ J g^{-1}.

in Fig. 7. The enthalpy of hydridation increases with the number of treatments and values of $-\Delta H$ of 52.6, 107.0 and 111.0 J g^{-1} are obtained for the first, second and third hydridations, respectively. In the first hydridation an endo minimum appears clearly at 481 °C, similar to the hydridation of the loose powder.

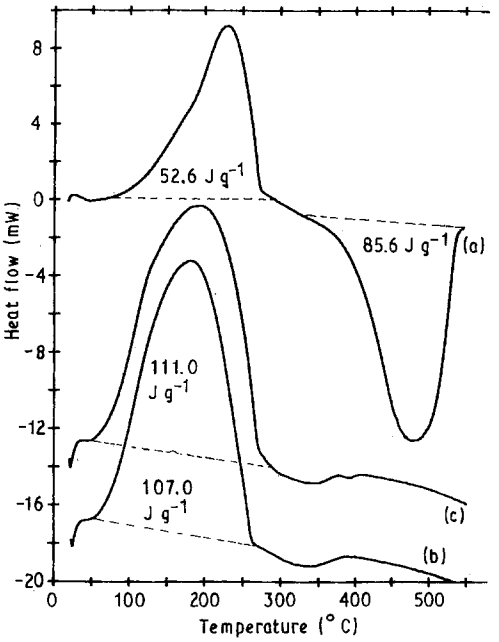

Figure 7 DSC thermograms of hydridation of pressed palladized powder.

3.4. Thermogravimetric measurements

The hydridation of a palladized sample was also followed by TGA. From the thermogram of Fig. 8a it is seen that an abrupt weight loss of some 9% takes place at about 490 °C, the temperature of the endothermal minimum of the DSC curves. Simultaneously, water vapour appears in the hydrogen stream, which must indicate that a reduction of the oxide film on the polycrystalline powder (formed by the heating at 500 °C of the sample during the initial palladization) is taking place. This explains the endo minimum of the DSC curve in Fig. 3, with an enthalpy change of 90.1 J g^{-1}.

After cooling the same sample in hydrogen and exposure to air for 30 min, similar to DSC measurements, and a subsequent hydridation under the same conditions, the TG thermogram shown in Fig. 8b is obtained. The first contact of the sample with the hydrogen flow is at 30 °C. A vigorous and fast reaction is obvious, with overheating of the sample to some 300 °C. After an initial small weight loss, the loop closes with a weight gain, increases further up to ~500 °C and experiences a sharp decrease afterwards. An identical thermogram is obtained for samples cooled in hydrogen, exposed to air and again hydridated.

After four hydridations in the TG cell, the sample cooled in hydrogen, after exposure to air for several hours, was hydridated again in the DSC cell. A curve almost identical to that in Fig. 3 was obtained. The enthalpy of hydridation of such a sample is, however, increased up to $\Delta H = -382$ J g^{-1}, as is that of the endo minimum, to which the reduction of the oxide film is ascribed ($\Delta H = 37$ J g^{-1}).

The original polycrystalline powder also behaves in a similar manner to the palladized sample during the TG analysis, but with a weaker effect. Fig. 9 shows the effects of triple hydridation with intermediate expo-

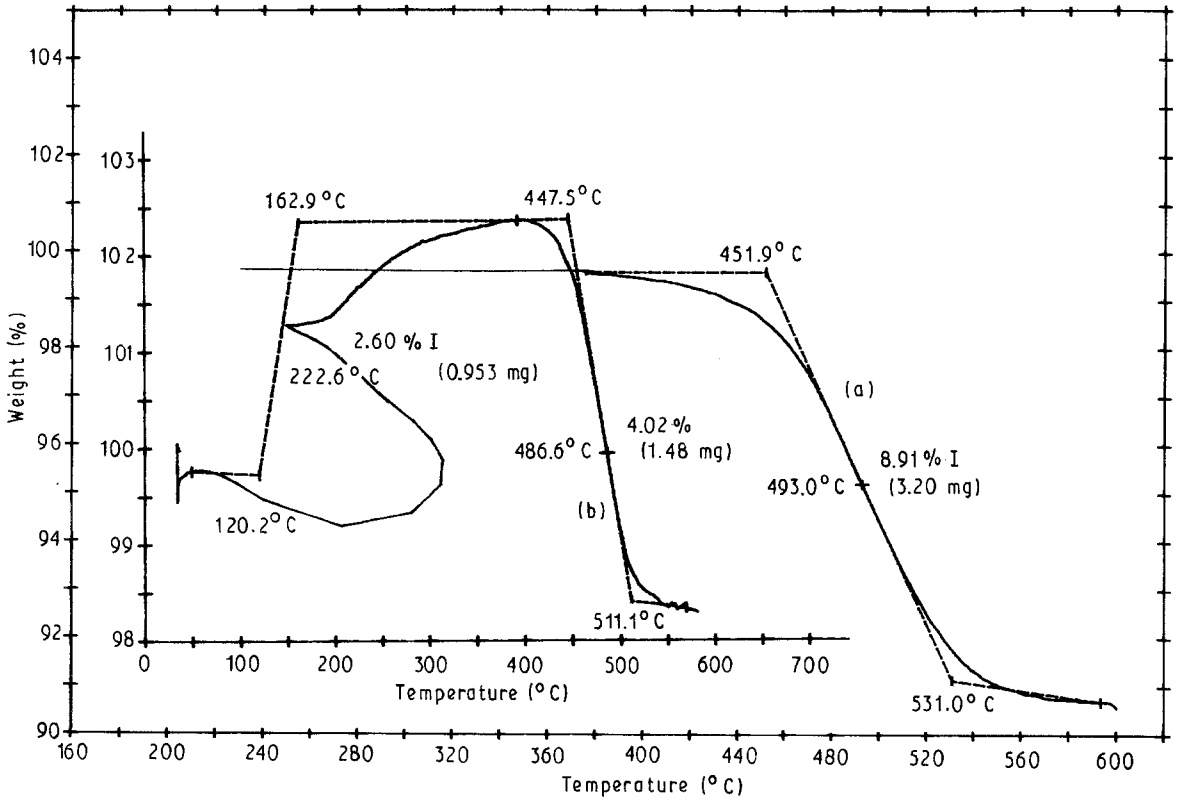

Figure 8 TG thermogram of the hydridation of the palladized powder in a hydrogen flow: (a) first and (b) second hydridation, 30 K min^{-1}.

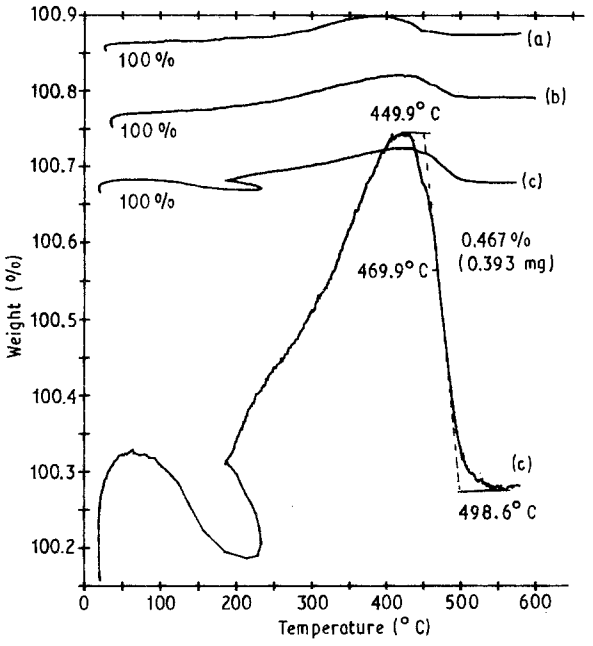

Figure 9 TG thermogram of hydridation of the original powder in a hydrogen flow: (a) first, (b) second and (c) third hydridation, 30 K min^{-1}. The lower curve (c) is the expanded upper one.

sures to air. The third hydridation shows overheating, the loop and subsequent weight loss.

Because the amount of palladium in the sample is insufficient to account for the total amount of absorbed hydrogen, and because of the thermal effect of $\Delta H = -382$ J g^{-1}, a hydrogen spillover process must have taken place.

3.5. Electrical resistance

Parallel to the thermal measurements, the specific electrical resistance of pressed samples of the original and palladized powders was examined. Measurements were performed in both air and a hydrogen atmosphere, in the range 20–600 °C. Repeated measurements were made on samples cooled in the respective atmosphere (air or hydrogen) and subsequently kept for 30 min in the open air. Tables I and II show values of the specific resistances at 600 and 20 °C, before and after heat treatment. Both tables show a considerable decrease in resistance on the first heating in air (which takes place around 350 °C). This decrease is 74-fold for the original sample and about 140-fold for the palla-

TABLE I Change of specific electrical resistance of pressed (9 kbar) original powder depending on the number of heating–cooling cycles in the interval 20–600 °C

No. of cycles	Gas flow	Resistance, ρ ($10^{-5}\ \Omega$ m)		
		20 °C, before heating	20 °C, after heating	At 600 °C
1	Air	56	0.74	0.74
2	Air	0.74	0.74	0.72
3	H_2	0.74	0.36	0.35
4	H_2	0.36	0.31	0.39
5	H_2	0.31	0.28	0.40

TABLE II Change of the specific electrical resistance of the pressed powder (9 kbar) depending on the number of heating–cooling cycles in the interval 20–600 °C

No. of cycles	Gas flow	Resistance, ρ (10^{-3} Ω m)		
		20 °C, before heating	20 °C, after heating	At 600 °C
1	Air	84	0.59	0.25
2	Air	0.59	0.58	0.24
3	H_2	0.58	0.07	0.03
4	H_2	0.07	0.04	0.05
5	H_2	0.04	0.04	0.04
6	H_2	0.03	0.03	0.04

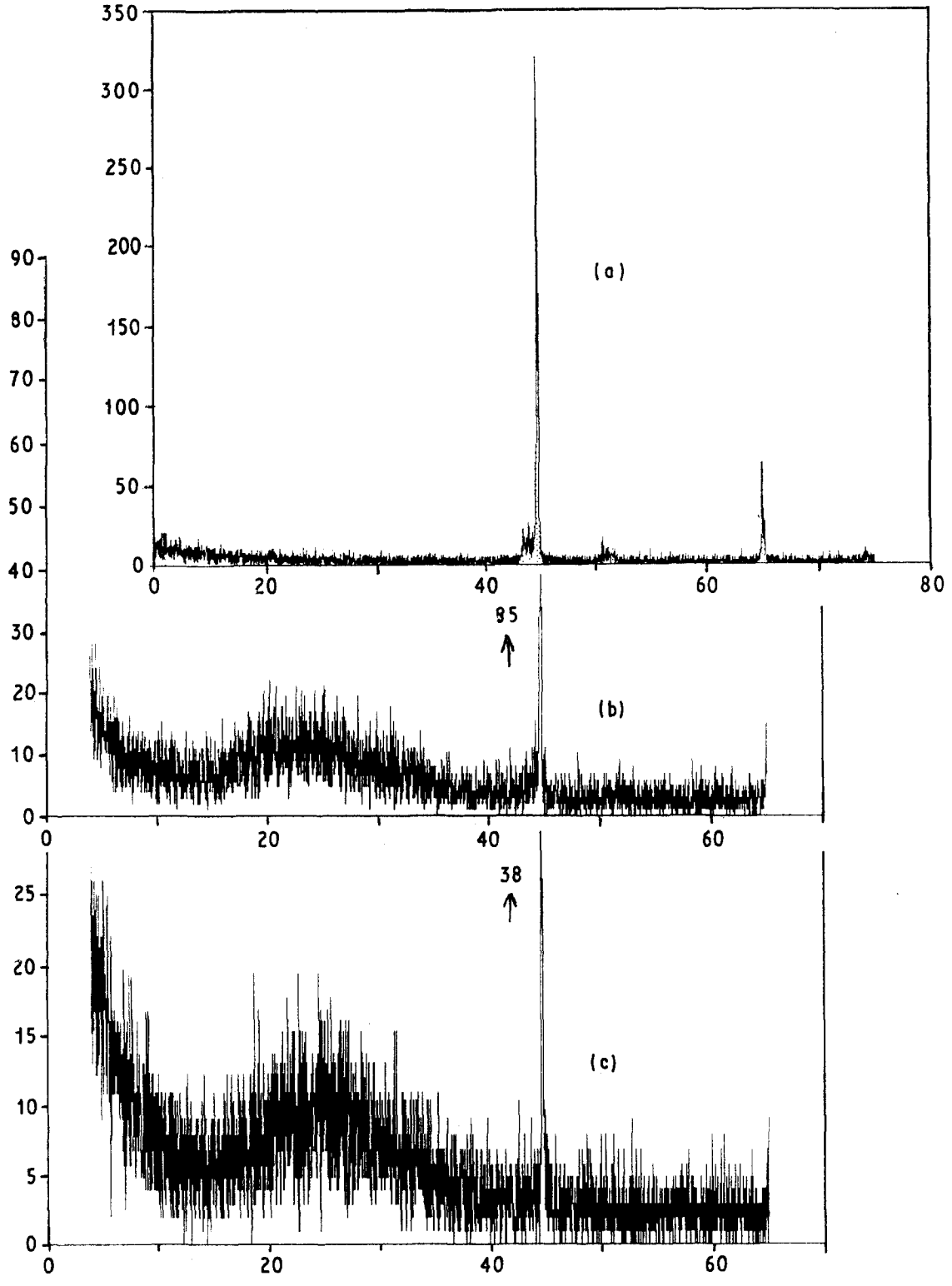

Figure 10 X-ray diffractograms of (a) the original powder, and the palladized powder (b) hydridated twice, (c) hydridated six times.

dized one. Repeated heating in air does not affect the resistance substantially. Heat treatments in hydrogen, however, because of the process of hydridation, lead to a further decrease, with a tendency towards a constant value after five to six cycles. The first hydridation of the original sample leads to a decrease in resistance of a factor of 2, while for the palladized sample this factor is 8, which is obviously the consequence of the hydrogen spillover effect.

3.6. X-ray diffraction

The X-ray diffraction patterns of the original powder compared to the hydridated ones show that the repeated hydridations lead to an increase in the content of the amorphous phase, with a decrease in the reflection of the crystal phase, as illustrated in Fig. 10.

4. Conclusion

The polycrystalline powder of the multicomponent alloy $FeNi_{1.75}Cu_{1.5}Mo_{0.5}$ absorbs hydrogen poorly in the range 170–250 °C. The addition of minute amounts of palladium (less than one part in 10^4) enhances hydrogen take-up considerably, in a reaction of the first order. The specific electrical resistances of samples of pure and palladized powders pressed at 9 kbar decrease considerably after heating in air or hydrogen up to 600 °C, tending to a constant value after repeated heating cycles. The decrease in resistance is much greater in hydrogen with samples containing palladium. The process of hydridation decomposes the crystal lattice leading to the amorphous state of the alloy. The main role of the absorption of hydrogen is ascribed to the hydrogen spillover effect.

References

1. G. G. LIBOWITZ and Z. BLANK, in "Solid State Chemistry in Energy Conversion and Storage", Advances in Chemistry Series 163, edited by J. B. Goodenough and M. S. Whittingham, (American Chemical Society, Washington, DC, 1977) pp. 271–83.
2. G. G. LIBOWITZ, *J. Nucl. Mater.* **2** (1960) 1.
3. J. JENSEN, "Energy Storage" (Newnes-Butterworths, London, 1980) pp. 25-30.
4. P. HAGENMULLER, in "Solid State Chemistry in Energy Conversion and Storage", Advances in Chemistry Series 163, edited by J. B. Goodenough and M. S. Whittingham (American Chemical Society, Washington, DC, 1977) pp. 1–13.
5. L. G. BENNET, S. D. ARGUNER and J. S. HAWEIT, *Int. J. Hydrogen Energy* **11** (1986) 577.
6. F. PAUSARIAN and W. E. WALLACE, *ibid.* **11** (1986) 789.
7. O. A. SERMON and G. C. BOND, *J. C. S. Faraday I*, **72** (1976) 730.
8. *Idem, ibid.* **76** (1980) 889.
9. M. V. ŠUŠIĆ and Y. M. SOLONIN, *Int. J. Hydrogen Energy* **16** (1991) 271.
10. *Idem, J. Mater. Sci.* **24** (1989) 3691.
11. W. E. WALLACE, in "Metal Hydrides", edited by G. Bambadakis (Plenum Press, New York, London, 1981).
12. H. J. BORCHARDT and D. FERRINGTON, *J. Amer. Chem. Soc.* **79** (1957) 41.

Received 25 September 1991
and accepted 11 August 1992